DOI: 10.1113/JP277727

Title: Long-term depression of presynaptic cannabinoid receptor function at parallel fiber synapses.

Running title: Activity-dependent plasticity of presynaptic Cb1 receptors.

Ying Yang[1,2], Tabita Kreko-Pierce[1], Rebecca Howell[1]*, and Jason R. Pugh[1,3]

1. University of Texas Health Science Center at San Antonio, Department of Cellular and Integrative Physiology, San Antonio, TX 78229

2. Xiangya School of Medicine, Department of Pain, The Third Xiangya Hospital and Institute of Pain Medicine, Central South University, Changsha, 410013, Hunan Province.

3. Center for Biomedical Neuroscience, University of Texas Health Science Center at San Antonio, San Antonio, Texas, 78229

*Present address: Oklahoma Medical Research Foundation & University of Oklahoma Health Science Center, Oklahoma City, OK 73104

Corresponding author:

Jason R. Pugh
Department of Cellular and Integrative Physiology
University of Texas Health Science Center San Antonio
7703 Floyd Curl Drive
South Texas Research Facility, MSC 8253
San Antonio, TX 78229-3900
210-567-1010
pughj@uthscsa.edu

Table of contents category: Neuroscience

Key words: cannabinoid receptor, parallel fiber, cerebellum, presynaptic, plasticity

Key Points:

- Inhibition of synaptic responses by activation of presynaptic cannabinoid type-1 (Cb1) receptors is reduced at parallel fiber synapses in the cerebellum following 4 Hz stimulation.
- Activation of adenylyl cyclase is necessary and sufficient for down-regulation of Cb1 receptors induced by 4 Hz stimulation.
- 4 Hz stimulation reduces Cb1 receptor function by 1) increasing the rate of endocannabinoid clearance from the synapse, 2) decreasing expression of Cb1 receptors.

Abstract

Cannabinoid type-1 receptors (Cb1R) are expressed in the presynaptic membrane of many synapses, including parallel fiber-Purkinje cell synapses in the cerebellum, where they are involved in short- and long-term plasticity of synaptic responses. We show that Cb1R expression itself is a plastic property of the synapse regulated by physiological activity patterns. We made patch-clamp recordings from Purkinje cells in cerebellar slices and assessed Cb1R activity by measuring depolarization-induced suppression of excitation (DSE). We find that DSE is normally stable at parallel fiber synapses, but following 4 Hz stimulation DSE is persistently reduced and recovers more rapidly. Using a combination of electrophysiology, pharmacology, and biochemistry, we show that changes in DSE are due to reduced expression of Cb1Rs and increased degradation of endocannabinoids by MAGL. Long-term changes in presynaptic Cb1R expression may alter other forms of Cb1R-dependent plasticity at parallel fiber synapses, priming or inhibiting the circuit for associative learning.

Introduction

In the field of synaptic plasticity, the majority of studies have focused on the role of postsynaptic receptors in increasing or decreasing synaptic strength, while very little is known about the modulation and composition of presynaptic receptors. One of the best known examples of a presynaptic receptor found widely throughout the brain is the cannabinoid type 1 receptor (Cb1), a G-protein coupled receptor activated by endocannabinoids. These receptors have been shown to be expressed at parallel fiber-Purkinje cell synapses in the cerebellum, where they inhibit release of glutamate in a process termed depolarization-induced suppression of excitation (DSE; Kreitzer and Regehr, 2001; Tanimura et al., 2009; Castillo et al., 2012). DSE occurs when the postsynaptic Purkinje cell is depolarized, triggering the synthesis of endocannabinoids which travel in a retrograde fashion to activate presynaptic Cb1 receptors. The activated Cb1 receptors inhibit voltage-gated calcium channels and reduce transmitter release. As endocannabinoids are cleared away from the synapse by diffusion and enzymatic digestion over 10s of seconds, transmitter release slowly returns to normal.

At parallel fiber synapses Cb1 receptor expression has been shown to vary greatly from synapse to synapse. Even consecutive boutons along a single parallel fiber may show significant differences in the Cb1 receptor-mediated inhibition of calcium channels (Zhang and Linden, 2009). The reason for this variability is not clear, though an intriguing possibility is that Cb1 receptor expression is regulated by circuit activity. Previous studies have shown plasticity of Cb1 receptors following pathophysiological stimuli such as, electroconvulsive therapy (Hill et al., 2007), seizures (Soltesz et al., 2015; Karlocai et al., 2011; Bojnik et al., 2012) spinocerebellar ataxia type-3 (Rodriguez-Cueto et al., 2016), and chronic treatment

with THC (Hirvonen er al., 2012; Burtson et al., 2010; Rubino et al., 2008), but to date, evidence for changes in presynaptic Cb1 receptor expression following physiological patterns of activity has been absent.

We show here that DSE at parallel fiber-Purkinje cell synapses is reduced and recovery from DSE is more rapid following 4 or 8 Hz parallel fiber stimulation. These changes are blocked by the presence of the adenylyl cyclase inhibitor, SQ-22536, and mimicked by bath application of the adenylyl cyclase activator, forskolin, indicating the necessity of adenylyl cyclase activation for reducing DSE. DSE is reduced through at least two mechanisms, an increase in clearance of the endocannabinoid 2-arachidonoylglycerol (2AG) from the synapse by the hydrolyzing enzyme monoacylglycerol lipase (MAGL), and reduced expression of presynaptic Cb1 receptors. In the presence of an MAGL inhibitor, 4 Hz stimulation no longer alters DSE amplitude or time course. And bath application of WIN 55,212-2, a Cb1 receptor agonist, produces less inhibition of transmitter release at synapses that were previously subjected to 4 Hz stimulation, indicating changes in Cb1 receptor signaling. Finally, we found decreased expression of CB1 receptors in cerebellar tissue exposed to forskolin using western blot analysis. These data demonstrate that Cb1 receptor expression in presynaptic terminals is a plastic property of parallel fiber synapses.

Methods

Ethical Approval All experimental procedures involving animals were approved by the Institutional Animal Care and Use Committee at the University of Texas Health Science Center San Antonio and followed the guidelines by the National Institutes of Health's *Guide for the Care and Use of Laboratory Animals*. All experiments were performed in accordance

with the principles and standards for reporting animal experiments in The Journal of Physiology (Grundy, 2015).

Slice Preparation Acute parasagittal brain slices were prepared from cerebella of male and female P14-25 C57BL/6 mice (Charles River, Wilmington, MA, USA). Prior to anesthesia and tissue collection all mice were given ad libitum access to food and water. Mice were deeply anesthetized by isoflurane inhalation before rapid dissection of the cerebellum in accordance with the University of Texas Health Science Center San Antonio protocols and guidelines. The cerebellum was immediately placed in ice-cold oxygenated (95% O_2, 5% CO_2) ACSF containing the following (in mM): 119 NaCl, 26.2 $NaHCO_3$, 2.5 KCl, 1.0 NaH_2PO_4, 11 glucose, 2 $CaCl_2$, 1.3 $MgCl_2$. Slices (200-300 µm) were cut from the vermis of the cerebellum with a vibratome (Leica Biosystems, Buffalo Grove, IL, USA) and incubated in oxygenated ACSF at 34°C for 30 min, and then at room temperature until they were transferred to a recording chamber.

Electrophysiology During recordings, slices were superfused with room temperature oxygenated ACSF at a flow rate of ~2 ml/min. Bath ACSF contained 100 µM picrotoxin (PTX, Abcam, Cambridge, MA, USA) and 3 µM CGP 55845 hydrochloride (Abcam, Cambridge, MA, USA) to block $GABA_A$ and $GABA_B$ receptors respectively, and isolate excitatory synaptic currents. Where indicated, ACSF also contained one of the following: 10 µM forskolin, 100 µM SQ-22536 (Tocris, Bristol, UK), 1 µM JZL 184 (Tocris, Bristol, UK), 30 µM Nimesulide (Sigma-Aldrich, St. Louis, MO, USA), 1 µM WIN 55,212-2 (Tocris, Bristol, UK).

Purkinje cells were visually identified and whole cell patch-clamp recordings were performed with borosilicate pipettes (2-4 MΩ). Access resistance was monitored throughout the experiment. Electrophysiological currents were recorded with a Multiclamp 700B

amplifier (Molecular Devices, Sunnyvale, CA, USA), filtered at 5 kHz and digitized at 50 kHz. Data were collected using pClamp software (Molecular Devices, Sunnyvale, CA, USA). EPSCs were evoked by stimulation of parallel fibers through a patch pipette filled with ACSF.

DSE protocol: Cells were held at -70 mV and EPSCs were stimulated at 0.5 Hz for 10 seconds to establish a baseline amplitude, cells were then depolarized to 0 mV for 1 or 2 seconds, after which the 0.5 Hz stimulation resumed for an additional 35-50 seconds. This DSE protocol was repeated either once per minute or every two minutes (results from these two conditions were indistinguishable and the data have been group together). The internal solution was composed of the following (in mM): 130 CsMeSO3, 10 CsCl, 10 HEPES, 0.5 EGTA, 2 MgCl2, 0.16 CaCl2, 2 QX-314, 4 Na-ATP, 0.5 Na-GTP (PH: 7.3-7.4, 280-300 mOsm). DSE was measured by comparing the amplitude of the first three EPSCs after Purkinje cell depolarization to the amplitude of baseline EPSCs. % inhibition during DSE was calculated by: % inhibition=$(1-EPSC_{DSE}/EPSC_{baseline})*100$. Recovery from DSE was measured by fitting an exponential curve to the EPSC amplitudes following Purkinje cell depolarization beginning with the third EPSC. Only cells in which the baseline EPSC amplitude and DSE amplitude were stable over the pre-stimulus period were included for further analysis (<10% change). Once a stable baseline of DSE was recorded for at least 5 minutes, parallel fibers were stimulated at 4 or 8 Hz for 30 seconds. Results following 4 or 8 Hz stimulation were similar and the data from these experiments was grouped in figure 1. Subsequent experiments were performed using only 4 Hz stimulation. Following 4/8Hz stimulation, the DSE protocol was resumed and DSE was measured for up to 40 minutes. In experiments using COX2/MAGL inhibitors, slices were incubated in the inhibitor for at least 40 minutes prior to

recording. In this case, DSE was induced once every 5-7.5 minutes as recovery from DSE was much slower in these conditions.

For two pathway experiments, independent parallel fiber pathways were stimulated by placing two stimulating electrodes in the molecular layer near the patched Purkinje cell. The stimulus intensity of each electrode was adjusted to evoke EPSCs in the Purkinje cell of roughly equal amplitude. Independence of the two pathways was determined by stimulating each pathway alone and then stimulating both pathways sequentially with a 20 ms interval. Pathways that did not show facilitation (<10%) when stimulated together were considered independent and used for subsequent experiments. For WIN 55,212-2 experiments, EPSCs from both pathways were recorded for 3-5 minute to establish that EPSCs were stable and of comparable amplitude. A 4 Hz stimulus (30 seconds) was then applied to one pathway and EPSCs from both pathways were again monitored for 5 minutes to again establish stable baseline amplitudes. 1 µM WIN 55,212-2 was then bath applied and EPSC amplitudes from both pathways were monitored for at least 15 minutes. In order to limit production of endocannabinoids in Purkinje cell dendrites a high EGTA internal solution was used in these experiments (in mM: 130 $CsMeSO_3$, 10 HEPES, 10 EGTA, 4 $MgCl_2$, 2 QX-314, 4 Na-ATP, 0.5 Na-GTP; PH: 7.3-7.4; 280-300 mOsm) and Purkinje cells were held at -70 mV throughout the experiment with no depolarizing steps.

For each cell, DSE and the rate of recovery from DSE were measured as the average values of all sweeps prior to 4 Hz stimulation and the average values of all sweeps 10 minutes after stimulation to the end of the recording. For experiments using WIN 55,212-2, EPSC values were measured as the average response amplitude following 4 Hz stimulation but before WIN 55,212-2 application, and the average of all response amplitudes from 10 minutes after

WIN 55,212-2 application to the end of the recording. CV2 was measured before and after 4/8Hz stimulation or forskolin application using the amplitudes of the baseline EPSCs prior to Purkinje cell depolarization. All data were acquired using P-Clamp10 software (Molecular Devices, Molecular Devices, Sunnyvale, CA, USA) and analyzed using IgorPro (Wavemetrics, Lake Oswego, OR, USA) using the Neuromatic plug-in (Rothman and Silver, 2018) and Excel (Microsoft, Redmond, WA, USA). Statistical significance was determined using paired Student's t-test and P-values≤0.05 were considered statistically significant. Data are reported as mean ± SE. Stimulus artifacts have been digitally removed from all current traces for clarity.

CB1-R protein quantification after forskolin treatment. *Membrane preparation:* After decapitation, cerebellar vermis from C57/BL6 mice were dissected, sliced in the sagittal plane, and incubated in either control ACSF or ACSF containing 10 µM forskolin. In both conditions ACSF was constantly bubbled with CO_2/O_2 during the incubation period. Three C57/BL6 mice were used per condition. Immediately following the incubation, tissue was homogenized in 500 µl of lysing buffer (50 mM Tris-HCl, pH 7.4, 1 mM EGTA, 1% Triton × -100, 250 mM sucrose, protease inhibitor cocktail, 1% phosphatase inhibitor cocktail). Extracts were cleared by centrifugation (1,000 x g for 10 min at 4 °C) and the resulting supernatant was removed and centrifuged at 115,000 rpm for 1 hr at 4 °C in a TLA120.2 (Beckman Coulter, Brea, CA). The pellet was resuspended in lysing buffer containing 50 mM Tris-HCl, pH 7.4, 1 mM EGTA, 1% Triton × -100, protease inhibitor cocktail (Roche, Basel Switzerland), 1% phosphatase inhibitor cocktail (Sigma-Aldrich, St. Louis, MO, USA).

Preparation of Synaptic Plasma Membrane (SPM): Synaptic plasma membranes were prepared as described in (Bermejo M.K et al. 2014). Briefly, after 10 min treatment in either

ACSF or ACSF + 10 µM forskolin (see above for details), slices of cerebellar vermis (7 mice for each condition) were homogenized in 0.32M sucrose, 4 mM HEPES, pH 7.3 buffer (buffered sucrose solution) with glass-Teflon tissue homogenizer (IKA, Wilmington, NC) at 900 rpm (12 stroked over a 30 sec period). The homogenates were centrifuged at 900 x g for 10 min at 4 °C yielding the supernatant (S1). S1 was then centrifuged at 10,000 x g for 15 min at 4 °C and the resulting crude synaptosomal fraction pellet (P2) was resuspended in 0.32 M HEPES buffered sucrose solution. The resuspended P2 was centrifuged at 10,000 x g for 15 min at 4 °C resulting in a washed crude synaptosomal pellet (P2'). The P2' was lysed in ddH2O and homogenized by hand with 3 strokes in a glass-Teflon tissue homogenizer after which the samples were adjusted back to 4 mM HEPES. The samples where then left to rotate at 4 °C for 30 min to ensure complete lysing. After 30 min the samples where centrifuged at 25,000 x g at 4 °C and the resulting synaptosomal membrane fraction (P3) was resuspended in 0.32 M HEPES-buffered sucrose solution. The resuspended P3 was layered carefully on top of the prepared discontinuous sucrose gradient. The gradients were balanced inside the buckets of the swinging bucket-rotors with 0.32 M HEPES-buffered sucrose and ultracentrifuged in a swinging bucket rotor (SW-41 Ti, Beckman Coulter, Brea, CA) at 150,000 x g for 2 hr at 4 °C. The synaptic plasma membrane (SPM) layer visible at the bottom of the 1.0 M/1.2M HEPES-buffered sucrose solution interphase was carefully withdrawn using a P200. The collected SPM layers were placed into a 3.5 ml thick-wall centrifuge tube and exactly 2.5 volumes of 4 mM HEPES were added to adjust the sucrose concentration to 0.32M. The samples were then ultracentrifuged in a fixed angle rotor (TLA-100.3, Beckman Coulter, Brea, CA) at 200,000 x g for 30 min at 4 °C. The resulting synaptic plasma membrane pellet (SPM) was resuspended in 50 mM HEPES/2 mM EDTA solution. All of the solutions used during

isolation of SPM where supplemented with protease (Roche, Basel Switzerland) and phosphatase (Thermo Fisher Scientific, Rockford, IL) inhibitor cocktails.

Western blots: Prior to gel loading total protein amounts were determined using PierceTM 660 nm protein assay (Thermo Fisher Scientific, Rockford, IL). Protein isolated by membrane preparation was diluted (1:1) in 2X sample buffer (100 mM Tris 6.8, 20% glycerol, 4% SDS) containing 10% β-mercaptoethanol, while protein isolated by synaptosomal preparation was diluted in 5X sample buffer (250 mM Tris 6.8, 50% glycerol, 10% SDS) containing 10% β-mercaptoethanol and samples were then boiled for 10 min. 40 µg (membrane preparation) or 30 µg (synaptosomal preparation) of protein were loaded in each well and subjected to SDS-PAGE using 12% Tris-HCl or gradient gels (Bio-Rad, Hercules, CA) and transferred to nitrocellulose membranes. The membranes were blocked with 5% milk in 0.1% Tween 20, TBS (pH 7.4) at RT for 1 hour. The membranes were initially probed with primary rabbit anti-CB1 polyclonal antibody (1:200) (Thermo Fisher Scientific, Rockford, IL) and secondary goat anti-rabbit HRP antibody (1:2500) (Santa Cruz Biotechnology, Dallas, TX). Hydrogen peroxide was used to inactivate secondary antibody. Blots were reblotted with primary mouse anti-tubulin antibody (1:30,000) (Developmental Studies Hybridoma Bank, Iowa City, IA) or mouse anti-β-actin (1:5000) (Sigma-Aldrich, St. Louis, MO, USA) and secondary goat anti-mouse antibody (1:2500) (Santa Cruz Biotechnology, Dallas, TX). For CB1-R antibody validation, cerebellar vermis from control (C57/BL6) and CB1-R KO mice (a kind gift from Xu-Friedman lab, University of Buffalo, NY) were used and the tissue and protein were processed as described above. Immunostained proteins were visualized using ECL detection method and band intensity was analyzed using Image J (NIH). Band intensity for each lane was normalized to its tubulin (membrane preparation) or β-actin (synaptosome

preparation) intensity value. Averages of normalized data were analyzed by unpaired student's t-test (excel). P values ≤0.05 were considered statistically significant.

Results

In order to assess presynaptic Cb1 receptor activity we measured depolarization induced suppression of excitation (DSE) at parallel fiber-Purkinje cell synapses (Kreitzer and Regehr, 2001). We made whole-cell voltage-clamp recordings from Purkinje cells in acute cerebellar slices and evoked EPSCs by electrical stimulation of parallel fibers in the molecular layer. Parallel fibers were stimulated at 0.5 Hz for 10 seconds to establish a baseline EPSC amplitude, the Purkinje cell was then depolarized by current injection through the patch pipette from -70 mV to 0 mV for 1 second, and parallel fibers were again stimulated at 0.5 Hz for 40 seconds (figure 1A). Following the depolarization EPSC amplitudes were substantially reduced (230.2±25.2 pA versus 84.4±25.9 pA, n=10, $p<0.0001$, figure 1A), consistent with previous findings (Kreitzer and Regehr, 2001; Brenowitz and Regehr, 2003). This protocol was repeated over 10 minutes to establish stable baselines of EPSC amplitudes and inhibition during DSE (figure 1B, C). After establishing this baseline, parallel fibers were stimulated at 4 or 8 Hz for 30 seconds, and the DSE protocol was again repeated over 30-40 minutes to monitor changes in DSE. Following 4 or 8 Hz stimulation, we observed a transient increase in baseline EPSC values (109.6±0.04% of control, n=10, p=0.04) and CV2 (p=0.058), consistent with previous reports of 4 or 8 Hz stimulation producing presynaptic potentiation at these synapses (Salin et al., 1996). In many cells, this was followed by a slow decrease in EPSC amplitudes (79.0±5.4% of control, figure 1B), likely due to post-synaptic long-term depression (LTD) elicited by repeated pairing of synaptic stimulation with Cb1R activation (Carey et al., 2011) in the protocol. Interestingly, inhibition of EPSCs during DSE

was reduced following 4/8 Hz stimulation (pre-4/8Hz stim: 66.4±5.6 % inhibition, post-4/8Hz stim: 56.8±5.4 % inhibition, n=10, p=0.02, figure 1 C, D, F). The reduction in DSE developed over 5-10 minutes following 4/8Hz stimulation and persisted for the duration of the recording. The change in DSE did not correlate with changes in baseline EPSC amplitudes (r^2=0.006), suggesting the change in DSE is not dependent on LTP/LTD at this synapse. In separate cells we repeated the DSE protocol over 25 minutes, but did not deliver a 4 or 8 Hz stimulus. In these cells DSE was stable over the duration of the recording (figure 1C, bottom) indicating the change in DSE is dependent on the 4/8 Hz stimulus and not simply due to buildup of endocannabinoids in the slice. In addition to reduced DSE, after 4/8Hz stimulation EPSC amplitudes recovered to their baseline values more rapidly following Purkinje cell depolarization ($\tau_{recovery}$: 21.7±2.9 vs 11.9±1.3 sec, n=10, p=0.001, figure 1D, E, G). Like the change in DSE, the change in recovery rate did not correlate with the change in EPSC amplitude across cells (r^2=0.024). In the absence of 4/8 Hz stimulation the recovery rate from DSE was stable over the course of 25 minutes (figure 1E, bottom). Results from 4 or 8 Hz stimulation were similar and have been grouped together for this experiment. In subsequent experiments only 4 Hz stimulation was used. These data demonstrate long-term changes in DSE at parallel fiber synapses following 4/8Hz stimulation, suggesting a novel form of synaptic plasticity. Many pre- and postsynaptic mechanisms could account for these changes in DSE, including reduced endocannabinoid production from the postsynaptic Purkinje cell, increased clearance of endocannabinoids from the synapse, reduced Cb1 receptor expression in the presynaptic bouton, or reduced downstream signaling from Cb1 receptors. We next investigated the mechanism(s) of long-term plasticity of DSE.

Activation of adenylyl cyclase reduces DSE

Previous studies have shown that 4 or 8 Hz stimulation activates adenylyl cyclase in parallel fiber boutons in the cerebellum (Salin et al., 1996; Rancillac and Crepel, 2004), suggesting that signaling through cAMP may be involved in the reduction of DSE. To test this possibility we repeated the same DSE protocol used in figure 1, but replaced the 4 Hz stimulation with a 10 minute bath application of foskolin, an adenylyl cyclase activator. Following forskolin application, we observe a significant potentiation of baseline EPSCs (221.9±16.6 versus 283.8±30.5 pA, n=7, p=0.028), as has been previously reported (Salin et al., 1996; Chen and Regehr, 1997; Bender et al., 2009), followed by a slow return to the baseline amplitude, likely due postsynaptic LTD. Following forskolin application, CV2 of EPSC amplitudes increased on average (117.8±17.3), but this change did not reach significance, likely due to limited number of EPSCs available for estimating CV2 in these experiments. Strikingly similar to results following 4/8 Hz, forskolin application reduced DSE (control: 69.6±5.5 % inhibition, forskolin: 55.8±7.0 % inhibition, n=7, p=0.006; Figure 2A-C) and increased the rate of recovery ($\tau_{recovery}$: 27.5±5.6 versus 11.6±1.5 ms, n=7, p=0.01; Figure 2B, C). In the same cells, we then delivered a 4 Hz parallel fiber stimulation and again measured DSE. In the presence of forskolin, 4 Hz stimulation had no further effect on DSE inhibition (53.3±5.3 % inhibition, n=7, p=0.5) or the rate of recovery (13.8±1.4 ms, n=7, p=0.2, figure 2A-C). These data show that (1) activation of adenylyl cyclase is sufficient to reduce DSE and increase recovery, and (2) the effects of 4 Hz stimulation on DSE are occluded by forskolin. Furthermore, in the presence of the adenylyl cyclase inhibitor SQ-22536 (100 µM) we did not observe a change in DSE inhibition (62.2±6.0 versus 61.5±6.4% inhibition, n=5, p=0.71) or rate of recovery (39.8±10.9 versus 41.2±12.5 sec, n=5, p=0.79) following 4 Hz stimulation (figure 2D-F). These

data demonstrate that activation of adenylyl cyclase is necessary and sufficient to reduce DSE and increase the rate of recovery from DSE.

Increased clearance of endocannabinoids

Previous work has shown that the rate of recovery from DSE is primarily dependent on the rate of clearance of endocannabinoids from the synapse by diffusion or enzymatic degradation (Straiker et al., 2011; Zhong et al., 2011; Liu et al., 2016). Therefore, the faster recovery from DSE observed following 4/8 Hz stimulation suggests a possible change in these clearance mechanisms. We first tested whether reducing endocannabinoid mobilization from Purkinje cells alone is sufficient to produce faster clearance and recovery from DSE. To alter endocannabinoid mobilization we measured DSE following 0.5, 1, or 2 second depolarization of the Purkinje cell. We found that increasing the duration of the depolarization increased inhibition during DSE (0.5 sec: 45.1±5.9 % inhibition, n=14; 1 sec: 65.8±2.2 % inhibition, n=59; 2 sec: 75.3±1.7 % inhibition, n=22, for all comparisons $p \leq 0.01$, unpaired student t-test), but did not significantly change the rate of recovery from DSE (0.5 sec: 22.3±3.9 sec; 1 sec: 19.2±3.6; 2 sec: 21.4±2.8 sec; for all comparisons $p > 0.5$, unpaired student t-test, figure 3A, B). In a subset of cells DSE was evoked with each duration of depolarization in the same cell. In these cells we also observed an increase in inhibition during DSE (0.5 versus 1 sec, p=0.06; 0.5 versus 2 sec, p=0.01, n=6, paired student t-test) but no change in the rate of recovery (0.5 versus 1 sec, p=0.99; 0.5 versus 2 sec, p=0.09, n=6, paired student t-test). These data suggest that increased rate of recovery from DSE following 4 Hz stimulation is not due to reduced endocannabinoid release; rather, there may be increased endocannabinoid clearance by enzymatic degradation.

Presynaptic Cb1 receptors at parallel fiber synapses are primarily activated by the endocannabinoid 2-AG with little or no activation by AEA (Safo and Regehr, 2005; Szabo et al., 2006; Wang et al., 2014; Liu et al., 2016). 2-AG is removed from the extracellular space through enzymatic hydrolysis and/or oxidation by enzymes (MAGL and COX-2) expressed in the presynaptic terminal (Vandevoode and Lambert, 2007; Gulyas et al., 2004; Straiker et al., 2011; Zhong et al., 2011; Liu et al., 2016). To test whether changes in these enzymes are responsible for the observed changes in DSE, we again measured DSE at parallel fiber-Purkinje cell synapses before and after 4 Hz stimulation, but in the presence of either the MAGL inhibitor jzl-184 or the COX2 inhibitor nimesulide. In the presence of jzl-184 recovery from DSE was greatly slowed compared to recovery in standard ACSF (jzl-184 $\tau_{recovery}$: 123.7±18.3 sec, n=15; p<0.001, figure 3C), confirming that hydrolysis of 2-AG by MAGL is largely responsible for the rate of recovery from DSE. Furthermore, following 4 Hz stimulation there was no change in inhibition (54.0±3.4 vs 56.8±3.6 % inhibition, n=15, p=0.18) or rate of recovery (123.7±18.3 vs 104.3±12.3 sec, n=15, p=0.14) of DSE (Figure 3C, D). In the presence of nimesulide recovery from DSE was also slower, though not to the extent seen in jzl-184 ($\tau_{recovery}$ 67.6±14.6 sec, n=12, p=0.02), and DSE was reduced following 4 Hz stimulation (70.7±3.1 versus 64.2±3.5 % inhibition, n=12, p=0.04), suggesting COX2 does not play a major role in altering DSE. These data indicate that increased clearance of endocannabinoids by MAGL contributes to the increased rate of recovery from DSE following 4 Hz stimulation, and may also contribute to reduced inhibition during DSE.

Reduction in DSE is independent of endocannabinoid production

We then tested whether the decrease in DSE observed following 4 or 8 Hz stimulation results from a decrease in production of endocannabinoids in the postsynaptic Purkinje cell.

To test this, we first recorded from Purkinje cells and stimulated two independent parallel fiber pathways (figure 4A). Independence of the two pathways was confirmed by stimulating each pathway alone and then stimulating the two pathways sequentially with a 20 ms inter-stimulus interval. Only cells that did not show facilitation (>10% increase) when both pathways were stimulated together were included for further analysis. We first tested whether the reduction in DSE following 4 Hz stimulation was pathway specific. During the 10 minute baseline period prior to 4 Hz stimulation DSE was similar in both pathways (64.6±6.0 versus 65.0±5.2 % inhibition, n=11). Interestingly, DSE was weakly correlated between the two pathways for individual cells (r^2=0.21), even though the level of DSE varied widely from cell to cell (~35-85% inhibition), suggesting there may also be cell wide control of DSE at parallel fiber synapses. 4 Hz stimulation was then delivered to one pathway (stim pathway), leaving the other unstimulated (cnt pathway). Following 4Hz stimulation DSE was significantly reduced in the stimulated pathway (56.1±4.5 % inhibition, n=11, p=0.02) but not the control pathway (60.1±6.1 % inhibition, n=11, p=0.08; figure 4B,C). Recovery from DSE was also faster in the stimulated pathway following 4 Hz stimulation (26.2±2.6 versus 19.5±2.3 seconds, n=11, p=0.002) but did not change in the control pathway (21.7±2.7 versus 19.6±2.4 seconds, p=0.38; figure 4D). The baseline recovery rate was not significantly different between the two pathways prior to 4 Hz stimulation (p=0.25). These data indicate that the changes in DSE following 4 Hz stimulation are specific to the stimulated synapses.

In order to test whether changes in cannabinoid signaling are dependent on changes in 2-AG production in Purkinje cells, we again recorded from Purkinje cells and stimulated two independent parallel fiber pathways. However, in this case depolarization of Purkinje cells and production of endogenous cannabinoids were replaced with exogenous application of

the Cb1 receptor agonist WIN 55,212-2. In these experiments a high EGTA (10 mM) internal solution (see methods) was used and depolarizing steps in the Purkinje cell were omitted to limit production and release of endocannabinoids from Purkinje cells. The stimulus intensity of each pathway was adjusted to give EPSCs of similar amplitude. After establishing a stable baseline EPSC amplitude in both pathways, 4 Hz stimulation was delivered to only one pathway (stim pathway), resulting in potentiation of EPSCs in this pathway (118.6±6.7% of baseline, n=8, p=0.036) but not in the other (control) pathway (99.9±5.0% of baseline, n=8, p=0.97). Following the 4 Hz stimulus (and potentiation of the stim pathway) EPSC amplitudes in both pathways were stable over a period of at least 5 minutes before applying WIN 55,212-2 (1 μM). WIN 55,212-2 inhibited EPSCs evoked by either pathway, but there was less inhibition of the stimulated pathway (cnt pathway: 60.7±6.6 % inhibition, stim pathway: 42.8±7.1 % inhibition, n=8, p=0.008, figure 5A). Inhibition of EPSCs by WIN 55,212-2 varied greatly across Purkinje cells, however, in every cell there was greater inhibition in the control pathway than in the stimulated pathway (figure 5B). From these data we conclude that Cb1 receptor-mediated inhibition of EPSCs can be reduced by 4 Hz stimulation independent of synthesis of endogenous cannabinoids. This suggests that reduction of DSE by 4 Hz parallel fiber stimulation involves down-regulation of Cb1 receptor signaling in the presynaptic terminal.

Reduced Cb1 receptor expression

Our data so far suggests that 4 or 8 Hz stimulation activates adenylyl cyclase, which has two downstream effects, an increase in endocannabinoid clearance by MAGL and reduced signaling through Cb1 receptors. Previous work has shown that Cb1 receptors can be internalized (Hsieh et al., 1999; Coutts et al., 2001; Leterrier et al., 2006) and are

subsequently degraded rather than recycled to the membrane (Martini et al., 2007). This raises the possibility that there is reduced CB1 receptor expression at parallel fiber synapses following 4 or 8 Hz stimulation. To directly measure changes in expression of Cb1 receptors in the cerebellar cortex we performed western blot analysis. To validate the specificity of the antibody, we first measured expression of Cb1 receptors from the cerebellar vermis of wild-type and Cb1 receptor knockout mice. Tissue from wild-type mice displayed a band of the approximate size expected for Cb1 receptors (~60 kD) that was absent from tissue from Cb1 receptor knockout mice (figure 6A). To test for changes in Cb1 receptor expression, we made acute slices from the cerebellar vermis of wild-type mice and incubated them either in oxygenated ACSF or ACSF containing forskolin for 10 minutes (the same duration of forskolin exposure used in physiology experiments, figure 2). In the whole membrane preparation, immunoblot analysis showed reduced Cb1 receptor protein in tissue exposed to forskolin compared to tissue incubated in ACSF alone (ACSF: 0.19±0.05, forskolin: 0.08±0.01, n=4, p-value=0.01; Figure 6B, C). In order to measure Cb1 receptor protein levels specifically at synapses, we isolated synaptosomes from cerebellar tissue exposed to standard ACSF or forskolin. Cb1 receptor protein was also reduced in synaptosomes obtained from tissue exposed to forskolin compared to control (ACSF: 0.59±0.09, forskolin: 0.37±0.07, n=8, p=0.06; figure 6D and E). These data show that Cb1 receptor expression is reduced in the cerebellar cortex following exposure to forskolin, consistent with internalization of Cb1 receptors at parallel fiber synapses. This suggests that reduction of DSE by 4 Hz stimulation is due, at least in part, to reduced expression of Cb1 receptors at parallel fiber synapses.

Discussion

Activation of presynaptic Cb1 receptors at parallel fiber-Purkinje cell synapses results in inhibition of transmitter release lasting 10s of seconds (DSE). We find that 4 Hz stimulation of parallel fibers reduces inhibition during DSE and increases the rate of recovery from DSE. Activation of adenylyl cyclase is sufficient to produce the same changes in DSE and occludes the effects of 4 Hz stimulation. Further, we find that 4 Hz stimulation reduces DSE through two complimentary mechanisms, increased clearance of endocannabinoids by MAGL, and decreased expression of Cb1 receptors in the presynaptic bouton.

Plasticity of endocannabinoid signaling

Previous studies have reported changes in Cb1 receptor activity under specific conditions. For instance, many studies have shown agonist induced desensitization and internalization of Cb1 receptors (Jin et al., 1999; Hsieh et al., 1999; Daigle et al., 2008) leading to receptor degradation (Martini et al., 2007). Several lines of evidence suggest that reduced CB1 expression observed here is not due to desensitization. We did not observe a change in %inhibition or recovery rate of DSE in unstimulated cells (figure 1C, E), suggesting repeated induction of DSE (and mobilization of endocannabinoids) alone is not sufficient to alter Cb1 receptor expression. Furthermore, we observed less inhibition of EPSCs by a CB1 receptor agonist (WIN 55,212-2) in parallel fiber pathways previously given a 4 Hz stimulation comparted to unstimulated control pathways (figure 5). In this experiment Cb1 receptor function is reduced in the stimulated pathway without prior exposure to endocannabinoids or Cb1 agonist, making agonist induced desensitization an unlikely mechanism. However, it is possible that some of the same pathways and phosphorylation sites identified in studies of desensitization contribute to activity-dependent internalization observed here.

Desensitization and internalization of Cb1 receptors can be initiated by activation of G-protein coupled receptor (GPCR) kinases (GRKs) and subsequent activation of β-arrestins (Jin et al., 1999; Kouznetsova et al., 2002). Several lines of work have shown that PKA can also phosphorylate and enhance the activity of GRK2 (Cong et al., 2001; Li et al., 2006; Kelly et al., 2008), raising the possibility that activity-dependent activation of adenylyl cyclase and its downstream target, PKA, results in internalization of Cb1 receptors through GRKs and β-arrestins in our experiments. On the other hand, several groups have shown that PKA and PKC can directly phosphorylate many GPCRs resulting in receptor internalization (Benovic et al., 1985; Hardy et al., 2005; Cho et al., 2007; Mathiesen and Ramirez, 2006), possibly including Cb1 receptors (Sim-Selley, 2003). Future work will be required to determine which, if either, of these mechanisms links adenylyl cyclase activity with Cb1 receptor internalization at parallel fiber synapses.

Several studies have also observed changes in Cb1 signaling following pathophysiological activity. For example, elevation of CB1 receptor expression in the hippocampus of rodent models of epilepsy (Karlocai et al., 2011; Bojnik et al., 2012) and in patients with temporal lobe epilepsy (Goffin et al., 2011) has been observed, suggesting epileptiform activity may increase Cb1 receptor expression. Likewise, febrile seizures (Chen et al., 2003) or tetanic stimulation of Schaffer collateral synapses in the hippocampus (Chen et al., 2007) result in increased depolarization-induced suppression of inhibition (DSI) in CA1 pyramidal cells, with no change in DSE. Interestingly, in these studies the increase in DSI was associated with a slower recovery from inhibition. This is consistent with our observation that reduced DSE was associated with faster recovery (figure 1), suggesting similar mechanisms may be involved in Cb1 receptor plasticity at these two very different synapses. However, unlike our

results, Chen et al. only saw changes in Cb1 receptor expression following high-frequency tetanic stimulation. Weaker, more physiological patterns of synaptic stimulation tested did not result in changes in DSI, suggesting seizure-like network activity is necessary for Cb1 receptor plasticity in the hippocampus. As far as we are aware, the present work is the first to show activity-dependent plasticity of presynaptic Cb1 receptors following physiological patterns of activity.

Physiological consequences

It has been proposed that transient reduction of synaptic transmission at parallel fiber-Purkinje cell synapses by Cb1 receptor activation acts as a homeostatic break on parallel fiber input (Marcaggi and Attwell, 2005). 2-AG is produced and mobilized in Purkinje cells by two signaling mechanisms, activation of mGluR1 and a rise in intracellular calcium. mGluR1 in Purkinje cells is activated by spillover of glutamate during high-frequency parallel fiber activity, particularly when a cluster of neighboring fibers are activated together (Rancz and Hausser, 2006; Batchelor et al., 1994; Pachoud et al., 2014). Local mobilization of 2-AG in Purkinje cells reduces glutamate release from the activated parallel fibers by activating Cb1 receptors, potentially turning down input from highly-active parallel fibers (Marcaggi and Attwell, 2005). A reduction in Cb1 receptor expression, as seen in our experiments, would reduce this homeostatic mechanism and allow for a greater range of parallel fiber input to Purkinje cells. In other words, highly active parallel fiber pathways whose input would normally be turned down by Cb1 receptor activation, would not be (or there would be less reduction in their synaptic input), allowing greater control over Purkinje cell firing rate. This would increase the range over which granule cell firing is able to control Purkinje cell output.

Cb1 receptors are also highly involved in induction of long-term synaptic plasticity at parallel fiber Purkinje cell synapses (Heifets and Castillo, 2009; Marcoaggi, 2015). Most theories of cerebellar function suggest LTD at parallel fiber Purkinje cell synapses, induced by paired climbing fiber and parallel fiber stimulation (Sakurai, 1987; Coesmans et al., 2004), is a critical site of plasticity for cerebellar learning and information storage (Ito, 1972; Lisberger, 1998; Medina et al., 2000; Dean et al., 2010). However, postsynaptic LTD (and LTP) at this synapse is not present in Cb1 receptor knockout mice or in the presence of AM251, a Cb1 receptor antagonist (Safo and Regehr, 2005; Carey et al., 2011; Wang et al., 2014), indicating parallel fiber plasticity is Cb1 receptor-dependent. Furthermore, knocking out Cb1 receptors or systemic injection of Cb1 receptor agonists or antagonists impairs acquisition of delay eyeblink conditioned responses, a cerebellum-dependent form of learning (Kishimoto and Kano, 2006; Steinmetz and Freeman, 2010 & 2013). This suggest that a reduction in Cb1 receptor expression, as we observed following 4 Hz stimulation, may prevent or raise the threshold for induction of LTD and LTP at parallel fiber synapses. Plasticity of presynaptic Cb1 receptor expression could provide a mechanism by which certain parallel fiber pathways are primed for LTP/LTD induction (increased Cb1 receptor expression) or inhibited from further LTP/LTD (reduced Cb1 receptor expression). In this way, down-regulation of Cb1 receptors may help consolidate learned responses in the cerebellum by preventing further LTP/LTD at the modified synapses.

Conclusion

The function of postsynaptic receptors has been studied extensively; in comparison we are only just beginning to understand the role of presynaptic receptors. We show here a long-term down-regulation of Cb1 receptor function at parallel fiber synapses. Given the high

Cb1 receptor expression at parallel fiber synapses (Herkenham et al, 1990; Tsou et al., 1998) and that receptor plasticity is generally bidirectional, it is likely that physiological mechanisms remain to be uncovered to up-regulate Cb1 receptor function as well. The field of presynaptic receptor plasticity is still new with relatively few examples using physiological stimuli (Lauri et al., 2001; Clarke et al., 2014; Orts-Del'Immagine and Pugh, 2018). Many synapses in the central nervous system, including parallel fibers, express a wide range of presynaptic ionotropic and metabotropic receptors; it will be interesting to discover whether other classes of receptors in other brain regions also experience activity-dependent plasticity.

Additional information

Competing Interests:

The authors declare that they have no competing interests.

Author Contributions:

Y.Y., R.H., and J.R.P., conceived of and designed the study. Y.Y., T.K., and R.H. performed the experiments. Y.Y., T.K., R.H., and J.R.P. analyzed the data. J.R.P. wrote the first draft of the manuscript and all authors contributed to the final manuscript.

Funding:

This work was funded by an NIH grant (R01 NS092809) awarded to J.R.P.

Acknowledgements:

We thank members of the Pugh lab for helpful discussion and comments on this work. We thank Matthew Xu-Friedman for kindly providing cerebellar tissue from Cb1 receptor knockout mice.

References

Batchelor AM, Madge DJ, Garthwaite J. 1994. Synaptic activation of metabotropic glutamate receptors in the parallel fibre-Purkinje cell pathway in rat cerebellar slices. Neuroscience. 63(4):911-915.

Bender VA1, Pugh JR, Jahr CE. (2009) Presynaptically expressed long-term potentiation increases multivesicular release at parallel fiber synapses. J Neurosci. 29(35):10974-10978.

Benovic JL, Pike LJ, Cerione RJ, Staniszewski C, Yoshimasa T, Codina J, Caron MG, Lefkowitz RJ. 1985. Phosphorylation of the mammalian beta-adrenergic receptor by cyclic AMP-dependent protein kinase. Regulation of the rate of receptor phosphorylation and dephosphorylation by agonist occupancy and effects on coupling of the receptor to the stimulatory guanine nucleotide regulatory protein. J Biol Chem. 260:7094–7101.

Bermejo MK, Milenkovic M, Salahpour A, Ramsey AJ. (2014) Preparation of synaptic plasma membrane and postsynaptic density proteins using a discontinuous sucrose gradient. J Vis Exp. 3;(91):e51896.

Bojnik E, Turunç E, Armağan G, Kanıt L, Benyhe S, Yalçın A, Borsodi A. 2012. Changes in the cannabinoid (CB1) receptor expression level and G-protein activation in kainic acid induced seizures. Epilepsy Res. 99(1-2):64-68.

Brenowitz SD, Regehr WG. 2003. Calcium dependence of retrograde inhibition by endocannabinoids at synapses onto Purkinje cells. J Neurosci. 23(15):6373-6384.

Burston JJ, Wiley JL, Craig AA, Selley DE, Sim-Selley LJ. 2010. Regional enhancement of cannabinoid CB₁ receptor desensitization in female adolescent rats following repeated Delta-tetrahydrocannabinol exposure. Br J Pharmacol. 161(1):103-112.

Carey MR, Myoga MH, McDaniels KR, Marsicano G, Lutz B, Mackie K, Regehr WG. 2011. Presynaptic CB1 receptors regulate synaptic plasticity at cerebellar parallel fiber synapses. J Neurophysiol. 105(2):958-963.

Castillo PE, Younts TJ, Chávez AE, Hashimotodani Y. 2012. Endocannabinoid signaling and synaptic function. Neuron.76(1):70-81.

Chen C, Regehr WG. (1997) The mechanism of cAMP-mediated enhancement at a cerebellar synapse. J Neurosci. 17(22):8687-8694.

Chen K, Neu A, Howard AL, Földy C, Echegoyen J, Hilgenberg L, Smith M, Mackie K, Soltesz I. 2007. Prevention of plasticity of endocannabinoid signaling inhibits persistent limbic hyperexcitability caused by developmental seizures. J Neurosci. 27(1):46-58.

Chen K, Ratzliff A, Hilgenberg L, Gulyás A, Freund TF, Smith M, Dinh TP, Piomelli D, Mackie K, Soltesz I. 2003. Long-term plasticity of endocannabinoid signaling induced by developmental febrile seizures. Neuron. 39(4):599-611.

Cho EY, Cho DI, Park JH, Kurose H, Caron MG, Kim KM. 2007. Roles of protein kinase C and actin binding protein 280 in the regulation of intracellular trafficking of dopamine D3 receptor. Mol Endocrinol. 21:2242–2254.

Clarke VR, Molchanova SM, Hirvonen T, Taira T, Lauri SE. 2014. Activity-dependent upregulation of presynaptic kainate receptors at immature CA3-CA1 synapses. J Neurosci. 34(50):16902-16916.

Coesmans M, Weber JT, De Zeeuw CI, and Hansel C. 2004. Bidirectional parallel fiber plasticity in the cerebellum under climbing fiber control. Neuron 44:691-700.

Cong M, Perry SJ, Lin FT, Fraser ID, Hu LA, Chen W, Pitcher JA, Scott JD, Lefkowitz RJ. 2001. Regulation of membrane targeting of the G protein-coupled receptor kinase 2 by protein kinase A and its anchoring protein AKAP79. J Biol Chem. 276:15192–15199.

Coutts AA, Anavi-Goffer S, Ross SA, MacEwan DJ, Mackie K, Pertwee RG, Irving AJ. (2001) Agonist-induced internalization and trafficking of cannabinoid CB1 receptors in hippocampal neurons J. Neurosci., 21:2425-2433.

Daigle TL, Kwok ML, Mackie K. (2008) Regulation of CB1 cannabinoid receptor internalization by a promiscuous phosphorylation-dependent mechanism. J Neurochem. 106(1):70-82.

Dean P, Porrill J, Ekerot CF, Jörntell H. 2010.The cerebellar microcircuit as an adaptive filter: experimental and computational evidence. Nat Rev Neurosci. 11(1):30-43.

Goffin K, Van Paesschen W, Van Laere K. 2011. In vivo activation of endocannabinoid system in temporal lobe epilepsy with hippocampal sclerosis. Brain. 134:1033-1040.

Grundy D. 2015. Principles and standards for reporting animal experiments in The Journal of Physiology and Experimental Physiology. J Physiol 593, 2547–2549.

Gulyas AI, Cravatt BF, Bracey MH, Dinh TP, Piomelli D, Boscia F, Freund TF. 2004. Segregation of two endocannabinoid-hydrolyzing enzymes into pre- and postsynaptic compartments in the rat hippocampus, cerebellum and amygdala. Eur J Neurosci. 20:441-458.

Hardy AR, Conley PB, Luo J, Benovic JL, Poole AW, Mundell SJ. 2005. P2Y1 and P2Y12 receptors for ADP desensitize by distinct kinase-dependent mechanisms. Blood. 105:3552–3560.

Heifets BD, Castillo PE. 2009. Endocannabinoid signaling and long-term synaptic plasticity. Annu Rev Physiol 71: 283–306.

Herkenham M, Lynn AB, Little MD, Johnson MR, Melvin LS, de Costa BR, Rice KC. 1990. Cannabinoid receptor localization in brain. Proc Natl Acad Sci U S A. 87(5):1932-1936.

Hill MN, Barr AM, Ho WS, Carrier EJ, Gorzalka BB, Hillard CJ. 2007. Electroconvulsive shock treatment differentially modulates cortical and subcortical endocannabinoid activity. J Neurochem. 103(1):47-56.

Hirvonen J, Goodwin RS, Li CT, Terry GE, Zoghbi SS, Morse C, Pike VW, Volkow ND, Huestis MA, Innis RB. 2012. Reversible and regionally selective downregulation of brain cannabinoid CB1 receptors in chronic daily cannabis smokers. Mol Psychiatry. 17(6):642-649.

Hsieh C, Brown S, Derleth C, Mackie K. (1999) Internalization and recycling of the CB1 cannabinoid receptor. J Neurochem. 73:493-501.

Ito M. 1972. Neural design of the cerebellar motor control system. Brain Res., 40:80-84.

Jin W, Brown S, Roche JP, Hsieh C, Celver JP, Kovoor A, Chavkin C, Mackie K. (1999) Distinct domains of the CB1 cannabinoid receptor mediate desensitization and internalization. J Neurosci. 19(10):3773-3780.

Karlócai MR, Tóth K, Watanabe M, Ledent C, Juhász G, Freund TF, Maglóczky Z. 2011. Redistribution of CB1 cannabinoid receptors in the acute and chronic phases of pilocarpine-induced epilepsy. PLoS One. 2011;6(11):e27196.

Kelly E, Bailey CP, Henderson G. 2008. Agonist-selective mechanisms of GPCR desensitization. Br J Pharmacol. 153: S379–S388.

Kishimoto Y, Kano M. 2006. Endogenous cannabinoid signaling through the CB1 receptor is essential for cerebellum-dependent discrete motor learning. J Neurosci. 26(34):8829-8837.

Kouznetsova M, Kelley B, Shen M, Thayer SA. 2002. Desensitization of cannabinoid-mediated presynaptic inhibition of neurotransmission between rat hippocampal neurons in culture. Mol Pharmacol. 61:477–485.

Kreitzer AC, Regehr WG. 2001. Retrograde inhibition of presynaptic calcium influx by endogenous cannabinoids at excitatory synapses onto Purkinje cells. Neuron. 29(3):717-727.

Lauri SE, Bortolotto ZA, Bleakman D, Ornstein PL, Lodge D, Isaac JT, Collingridge GL. 2001. A critical role of a facilitatory presynaptic kainate receptor in mossy fiber LTP. Neuron. 32(4):697-709.

Leterrier C, Laine J, Darmon M, Boudin H, Rossier J, Lenkei Z. (2006) Constitutive activation drives compartment-selective endocytosis and axonal targeting of type 1 cannabinoid receptors. J. Neurosci., 26:3141-3153.

Li X, Huston E, Lynch MJ, Houslay MD, Baillie GS. 2006. Phosphodiesterase-4 influences the PKA phosphorylation status and membrane translocation of G-protein receptor kinase 2 (GRK2) in HEK-293beta2 cells and cardiac myocytes. Biochem J. 394:427–435.

Lisberger SG. 1998. Cerebellar LTD: a molecular mechanism of behavioral learning? Cell. 92(6):701-704.

Liu X, Chen Y, Vickstrom CR, Li Y, Viader A, Cravatt BF, Liu QS. 2016. Coordinated regulation of endocannabinoid-mediated retrograde synaptic suppression in the cerebellum by neuronal and astrocytic monoacylglycerol lipase. Sci Rep. 6:35829.

Marcaggi P, Attwell D. 2005. Endocannabinoid signaling depends on the spatial pattern of synapse activation. Nat Neurosci. 8(6):776-781.

Marcaggi P. 2015. Cerebellar endocannabinoids: retrograde signaling from purkinje cells. Cerebellum. 14(3):341-353.

Martini L, Waldhoer M, Pusch M, Kharazia V, Fong J, Lee JH, Freissmuth C, Whistler JL. (2007) Ligand-induced down-regulation of the cannabinoid 1 receptor is mediated by the G-protein-coupled receptor-associated sorting protein GASP1. FASEB J. 21(3):802-811.

Mathiesen JM, Ramirez MT. 2006. The metabotropic glutamate receptor 4 is internalised and desensitised upon protein kinase C activation. Br J Pharmacol. 148:279–290.

Medina JF, Nores WL, Ohyama T, and Mauk MD. 2000. Mechanisms of cerebellar learning suggested by eyelid conditioning. Current Opinion in Neurobiology 10:717-724.

Orts-Del'Immagine A, Pugh JR. 2018. Activity-dependent plasticity of presynaptic GABAB receptors at parallel fiber synapses. Synapse. 72(5):e22027.

Pachoud B, Sharma P, Bergerot A, Knöpfel T, Marcaggi P. 2014. Quantification of the density of cooperative neighboring synapses required to evoke endocannabinoid signaling. Neuroscience. 256:412-425.

Rancillac A, Crépel F. 2004. Synapses between parallel fibres and stellate cells express long-term changes in synaptic efficacy in rat cerebellum. J Physiol. 554:707-720.

Rancz EA, Häusser M. 2006. Dendritic calcium spikes are tunable triggers of cannabinoid release and short-term synaptic plasticity in cerebellar Purkinje neurons. J Neurosci. 26(20):5428-5437.

Rodríguez-Cueto C, Hernández-Gálvez M, Hillard CJ, Maciel P, García-García L, Valdeolivas S, Pozo MA, Ramos JA, Gómez-Ruiz M, Fernández-Ruiz J. 2016. Dysregulation of the endocannabinoid signaling system in the cerebellum and brainstem in a transgenic mouse model of spinocerebellar ataxia type-3. Neuroscience. 339:191-209.

Rothman JS and Silver RA (2018) NeuroMatic: An Integrated Open-Source Software Toolkit for Acquisition, Analysis and Simulation of Electrophysiological Data. Front. Neuroinform. 12:14.

Rubino T, Vigano' D, Realini N, Guidali C, Braida D, Capurro V, Castiglioni C, Cherubino F, Romualdi P, Candeletti S, Sala M, Parolaro D. 2008. Chronic delta 9-tetrahydrocannabinol during adolescence provokes sex-dependent changes in the emotional profile in adult rats: behavioral and biochemical correlates. Neuropsychopharmacology. 33(11):2760-2771.

Safo PK, Regehr WG. 2005. Endocannabinoids control the induction of cerebellar LTD. Neuron. 48(4):647-659.

Sakurai M. 1987. Synaptic modification of parallel fiber-Purkinje cell transmission in in vitro guinea-pig cerebellar slices. J. Physiol. 394:463-480.

Salin PA, Malenka RC, Nicoll RA. 1996. Cyclic AMP mediates a presynaptic form of LTP at cerebellar parallel fiber synapses. Neuron. 16(4):797-803.

Sim-Selley LJ. 2003. Regulation of cannabinoid CB1 receptors in the central nervous system by chronic cannabinoids. Crit Rev Neurobiol. 15(2):91-119.

Soltesz I, Alger BE, Kano M, Lee SH, Lovinger DM, Ohno-Shosaku T, Watanabe M. 2015. Weeding out bad waves: towards selective cannabinoid circuit control in epilepsy. Nat Rev Neurosci. 16(5):264-277.

Straiker A, Wager-Miller J, Hu SS, Blankman JL, Cravatt BF, Mackie K. 2011. COX-2 and fatty acid amide hydrolase can regulate the time course of depolarization-induced suppression of excitation. Br J Pharmacol. 164(6):1672-1683.

Steinmetz AB, Freeman JH. 2010. Central cannabinoid receptors modulate acquisition of eyeblink conditioning. Learn Mem.17(11):571-576.

Steinmetz AB, Freeman JH. 2013. Differential effects of the cannabinoid agonist WIN55,212-2 on delay and trace eyeblink conditioning. Behav Neurosci. 127(5):694-702.

Szabo B, Urbanski MJ, Bisogno T, Di Marzo V, Mendiguren A, Baer WU, Freiman I. 2006. Depolarization-induced retrograde synaptic inhibition in the mouse cerebellar cortex is mediated by 2-arachidonoylglycerol. J Physiol. 577:263-280.

Tanimura A, Kawata S, Hashimoto K, Kano M. 2009. Not glutamate but endocannabinoids mediate retrograde suppression of cerebellar parallel fiber to Purkinje cell synaptic transmission in young adult rodents. Neuropharmacology. 57(2):157-163.

Tsou K, Brown S, Sañudo-Peña MC, Mackie K, Walker JM. 1998. Immunohistochemical distribution of cannabinoid CB1 receptors in the rat central nervous system. Neuroscience. 83(2):393-411.

Vandevoorde S, Lambert DM. 2007. The multiple pathways of endocannabinoid metabolism: a zoom out. Chem Biodivers 4: 1858-2007.

Wang DJ, Su LD, Wang YN, Yang D, Sun CL, Zhou L, Wang XX, Shen Y. 2014. Long-term potentiation at cerebellar parallel fiber-Purkinje cell synapses requires presynaptic and postsynaptic signaling cascades. J Neurosci. 34(6):2355-2364.

Zhang W, and Linden DJ. 2009. Neurmodulation at single presynaptic boutons of cerebellar parallel fibers is determinded by bouton size and basal action potential-evoked Ca transient amplitude. J Neurosci 29:15586-15594.

Zhong P, Pan B, Gao XP, Blankman JL, Cravatt BF, Liu QS. 2011. Genetic deletion of monoacylglycerol lipase alters endocannabinoid-mediated retrograde synaptic depression in the cerebellum. J Physiol. 589:4847-4855.

Additional information:

Competing interest: The authors have no conflicts of interest.

Funding: This work was supported by a grant from the National Institute of Neurological Disorders and Stroke (NS092809).

Figure legends:

Figure 1. DSE is reduced and recovers more rapidly following 4/8 Hz stimulation. A. Top: Diagram of parallel fiber stimulation (stim) and Purkinje cell depolarization (Vstep) during DSE protocol. Bottom: Example current traces of EPSCs showing DSE. **B.** Average baseline EPSC amplitudes across the time-course of the experiment normalized to the average amplitude prior to 4/8 Hz stimulation. **C.** Top: Average inhibition during DSE normalized to the average DSE value prior to 4/8 Hz stimulation (t=0) across the time course of the experiment. Inset: Example traces of EPSCs before (black) and after (gray) Purkinje cell depolarization showing reduced DSE after 4 Hz stimulation. Bottom: Average inhibition during DSE over 25 minutes in cells that did not receive 4/8 Hz stimulation, showing that DSE is stable in unstimulated cells. **D.** EPSC amplitudes during the DSE protocol (normalized to the baseline amplitude before depolarization) before (black) or after (red) 4 Hz parallel fiber stimulation from the same cell. Exponential fit to the recovery from DSE and calculated recovery time-constants are shown. **E.** Top: Average time constant of recovery from DSE across the time course of the experiment. Bottom: Average recovery time constant of DSE over 25 minutes in cells that did not receive 4/8 Hz stimulation, showing that recovery from DSE is stable in unstimulated cells **F.** Average % inhibition during DSE before (black) and after (red) 4/8 Hz stimulation. Data from individual cells are plotted as connected gray markers. **G.** Average recovery time constant during DSE before (black) and after (red) 4/8 Hz stimulation. Data from individual cells are plotted as connected gray markers. (*) indicates p-value<0.05, (**) indicates p-value<0.01.

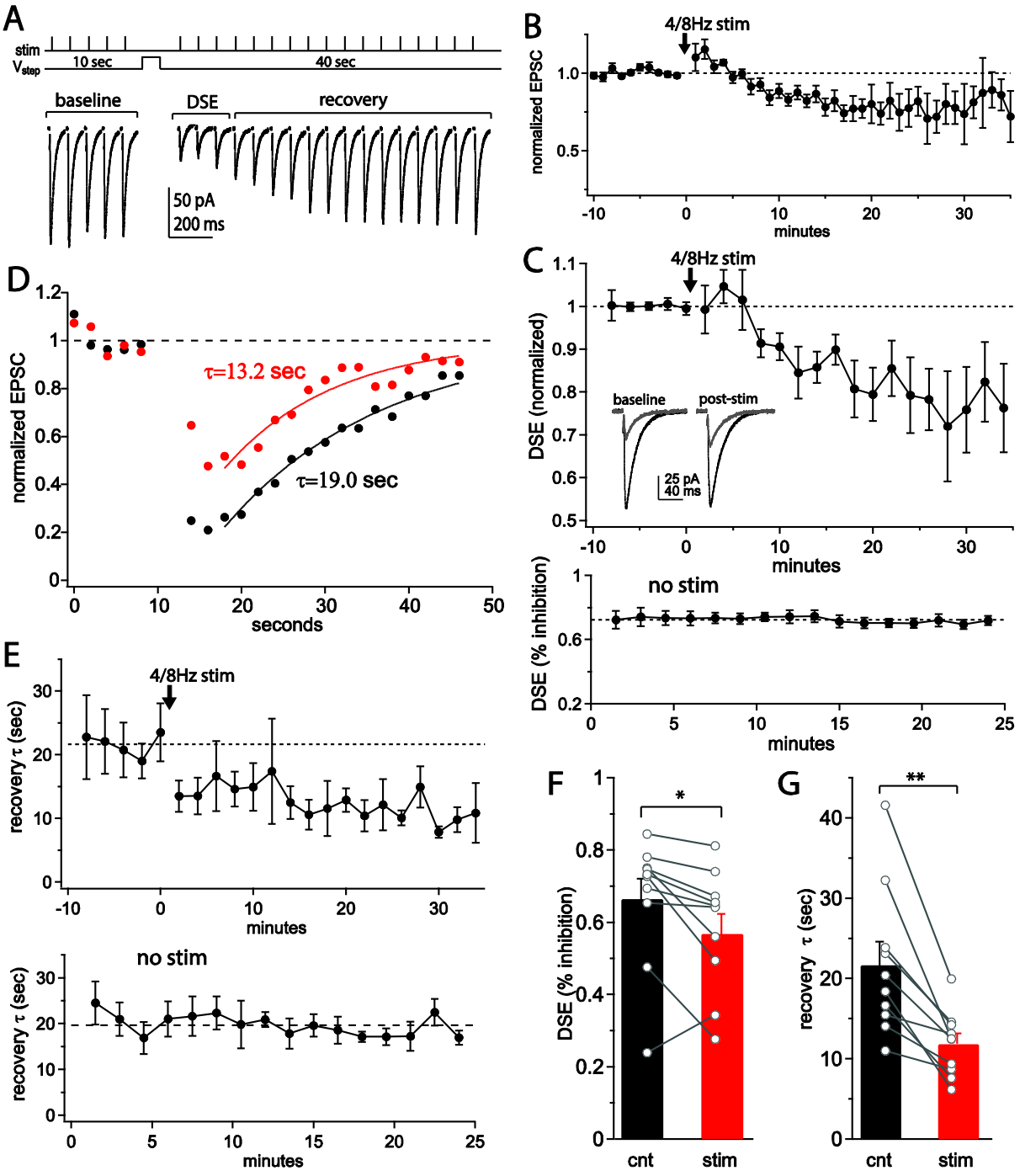

Figure 2: Activation of adenylyl cyclase is necessary and sufficient for changes in DSE. A. Example current traces of EPSCs before (black) and after (gray) Purkinje cell depolarization, showing extent of DSE in control, after bath application of forskolin, and after 4 Hz stimulation in the same cell. **B.** EPSC amplitudes during the DSE protocol (normalized to the baseline amplitude before depolarization) in control (black), during forskolin application (blue), and after 4 Hz stimulation (purple) in the same cell. Exponential fit to the recovery from DSE and calculated recovery time-constants are shown. **C.** Average % inhibition (left) and recovery time constant (right) during DSE in control (black), forskolin (blue), and following 4 Hz stimulation (purple). Data from individual cells are plotted as connected gray markers. **D.** Example current traces of EPSCs before (black) and after (red) Purkinje cell depolarization in the presence of SQ-22536 (an adenylyl cyclase inhibitor), showing extent of DSE in control and after 4 Hz stimulation in the same cell. **E.** EPSC amplitudes during the DSE protocol (normalized to the baseline amplitude before depolarization) in the presence of SQ-22536 in control (black) and after 4 Hz stimulation (red) in the same cell. **F.** Average % inhibition (left) and recovery time constant (right) during DSE in control (black) and following 4 Hz stimulation (red). Data from individual cells are plotted as connected gray markers. (*) indicates p-value<0.05, (**) indicates p-value<0.01, NS indicates p-value>0.05.

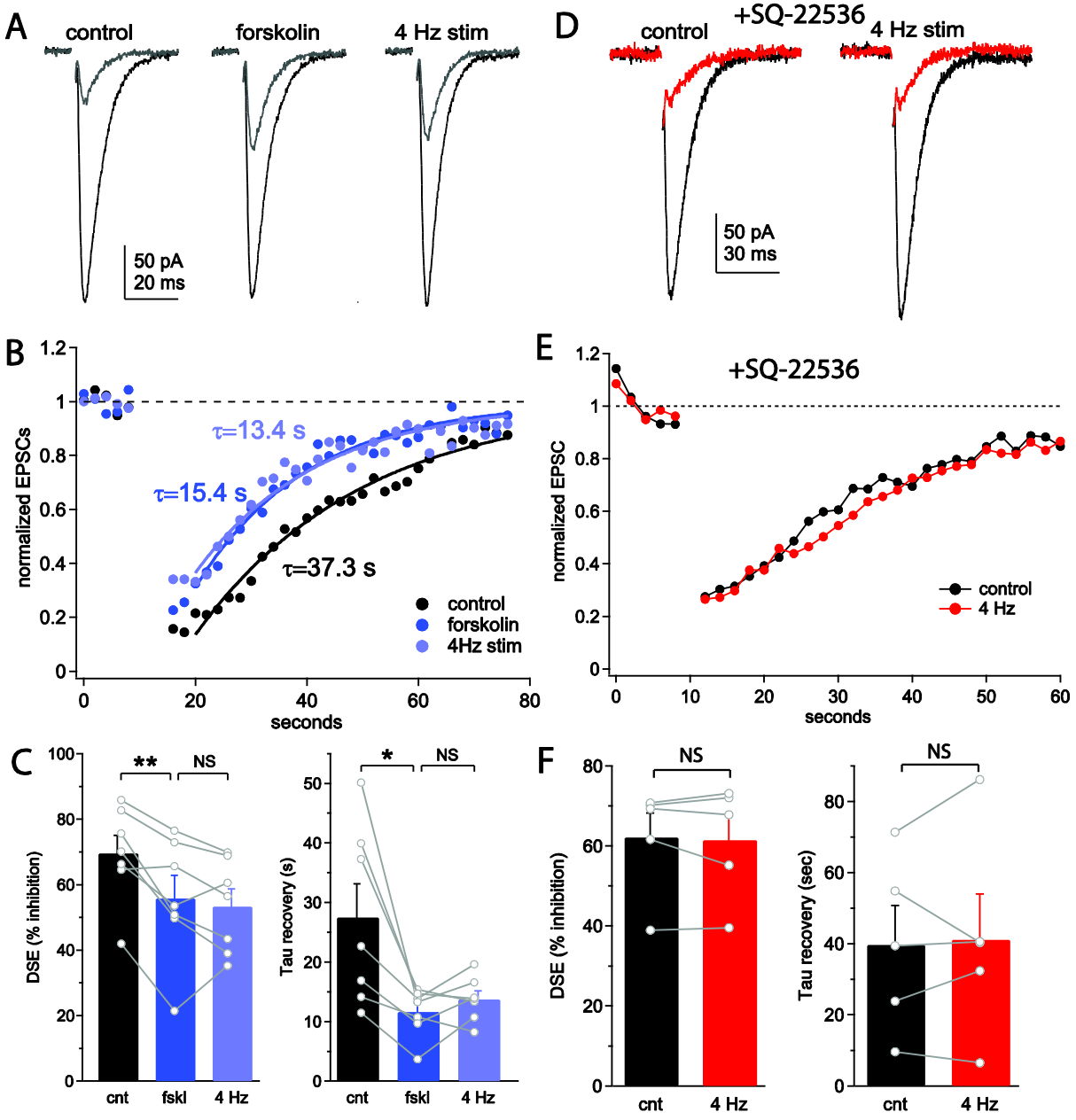

Figure 3. DSE is not altered by 4 Hz stimulation in the presence of MAGL inhibitor. A. EPSC amplitudes (normalized to the baseline amplitude) before and after DSE was induced by 0.5 second (blue), 1 second (black), or 2 second (gray) Purkinje cell depolarization in the same cell. Exponential fit to the recovery from DSE and calculated recovery time-constants are shown. **B.** Average % inhibition (left) and recovery time constant (right) of DSE following 0.5 second (blue), 1 second (black), or 2 second (gray) Purkinje cell depolarization. Data from individual cells are plotted as gray markers. **C.** Average EPSC amplitudes during the DSE protocol (normalized to the baseline amplitude) before (black) or after (red) 4 Hz stimulation in the presence of JZL-184. Inset: Example current traces of EPSCs in the presence of the MAGL inhibitor JZL-184 before (black/red) and after (gray/pink) Purkinje cell depolarization in the same cell. **D.** Average % inhibition (left) and recovery time constant (right) of DSE in control (black) and following 4 Hz stimulation (red) in JZL-184. Data from individual cells are plotted as connected gray markers. (*) indicates p-value<0.05, (**) indicates p-value<0.01, (***) indicates p-value<0.001, NS indicates p-value>0.05.

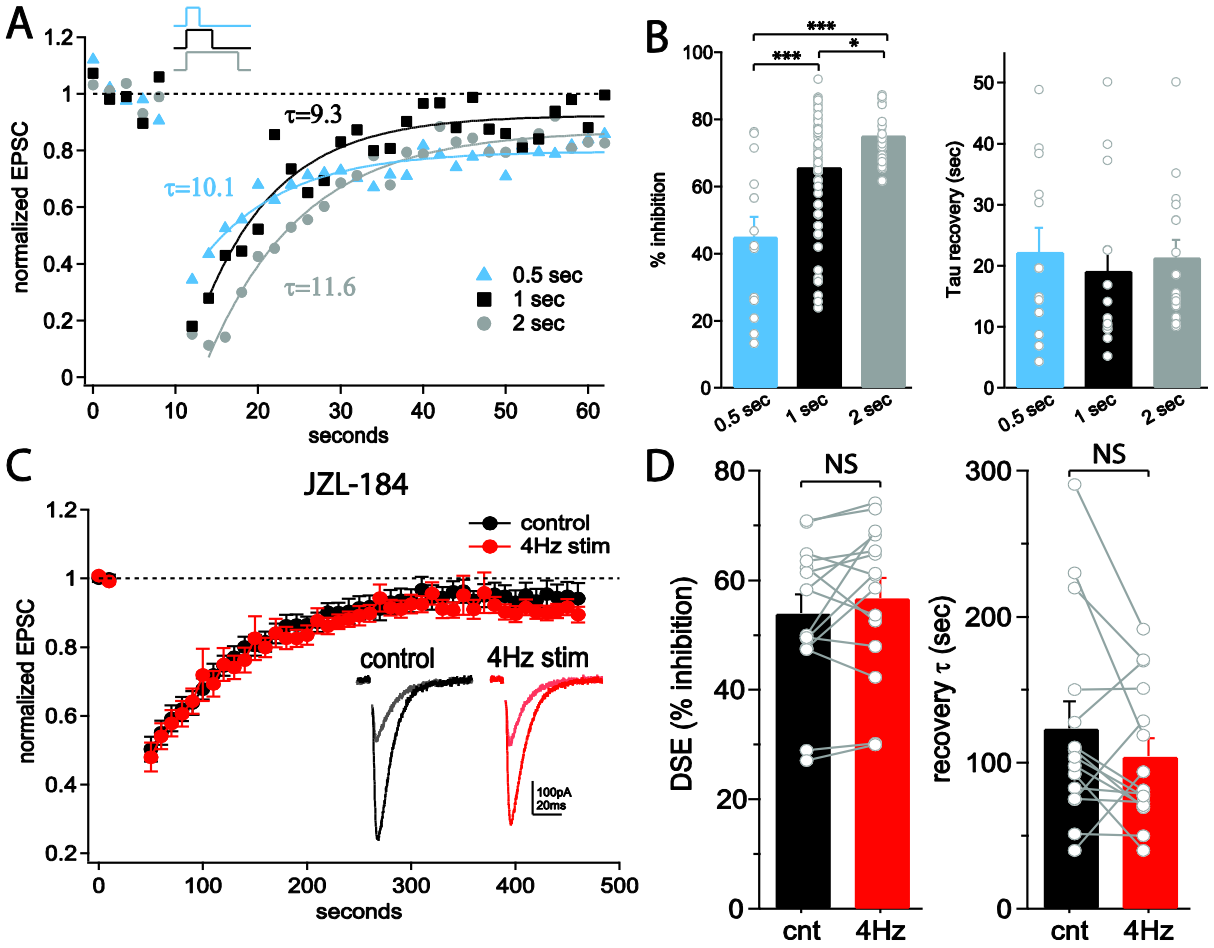

Figure 4. Reduction of DSE is pathway specific. A. Diagram of stimulating and recording electrode placement during two-pathway experiments. **B.** Example traces of EPSCs during the baseline period (black/red) and during DSE (gray/pink) before (black) or after (red) 4 Hz stimulation from the stimulated pathway (top) and control pathway (bottom). **C.** Average %-inhibition during DSE in the stimulated pathway and control pathway before (black) and after (red) 4 Hz stimulation. Data from individual cells are plotted as connected gray markers. **D.** Average recovery time constant in the stimulated pathway and control pathway before (black) and after (red) 4 Hz stimulation. Data from individual cells are plotted as connected gray markers. (*) indicates p-value<0.05, (**) indicates p-value<0.01, NS indicates p-value>0.05.

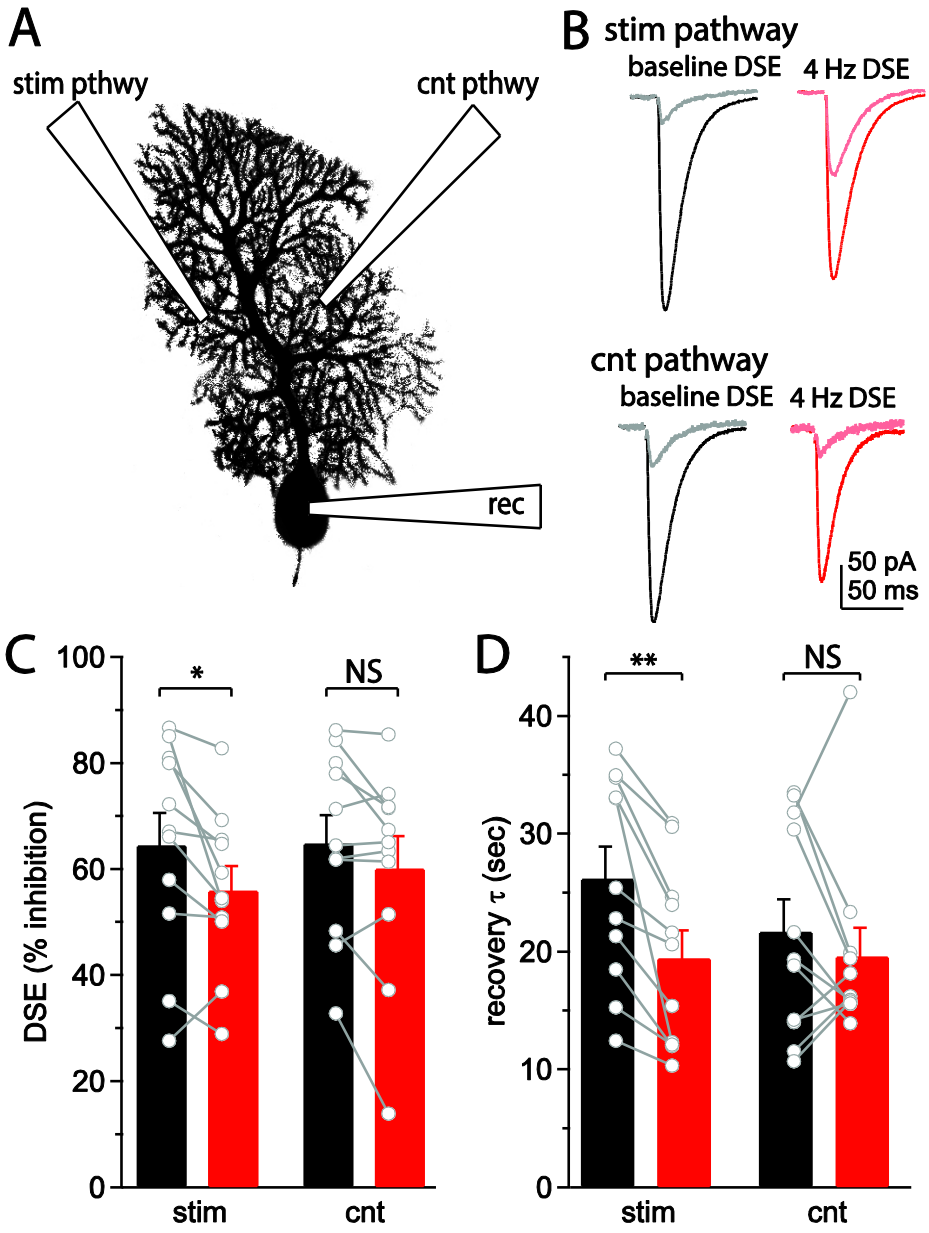

Figure 5. Reduction of DSE is independent of endocannabinoid production. A. Left: Normalized EPSC amplitudes from two independent parallel fiber pathways showing inhibition following bath application of WIN55,212-2. Right: Example traces of average EPSCs from the stimulated pathway (top) and control pathway (bottom) before (red/black) and after (pink/gray) WIN55,212-2 application. **B.** Average inhibition of the control and stimulated pathway by WIN55,212-2. Data from the same cells are plotted as connected gray markers. (**) indicates p-value<0.01.

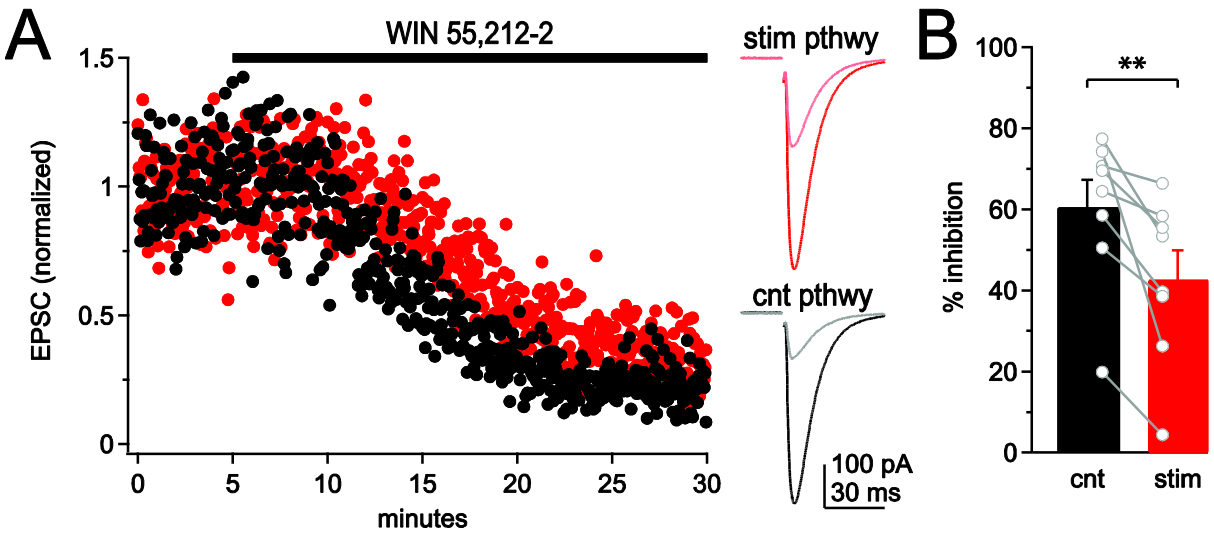

Figure 6. Cb1 receptor expression is reduced by forskolin. A. Immunoblot analysis of Cb1 receptor expression in cerebellar extracts from wild-type (CB1R-WT, lanes 1 and 2) and Cb1 receptor knockout tissue (CB1R-KO, lanes 3 and 4) probed with anti-Cb1 receptor antibody. Tubulin is shown as a loading control. **B.** Immunoblot analysis using a membrane preparation of Cb1 receptor expression from wild-type cerebellar tissue incubated for 10 minutes in either ACSF (-Fskl, lane 1 and 2) or in forskolin (+Fskl, lane 3 and 4). Immunoblots (from the same gel) of cerebellar tissue from Cb1R knockout mouse is also shown (lanes 5 and 6). Tubulin is shown as a loading control. **C.** Quantification of relative intensity of CB1 receptor expression (normalized to the intensity of tubulin) using the membrane preparation. **D.** Immunoblot analysis using a synaptosomal preparation of Cb1 receptor expression from wild-type cerebellar tissue incubated for 10 minutes in either ACSF (-Fskl, lane 1 and 2) or in forskolin (+Fskl, lane 3 and 4). β-actin is shown as a loading control. **E.** Quantification of relative intensity of CB1 receptor expression (normalized to the intensity of β-actin) using the synaptosomal preparation. Error bars indicate standard error. (*) indicates p-value<0.05.

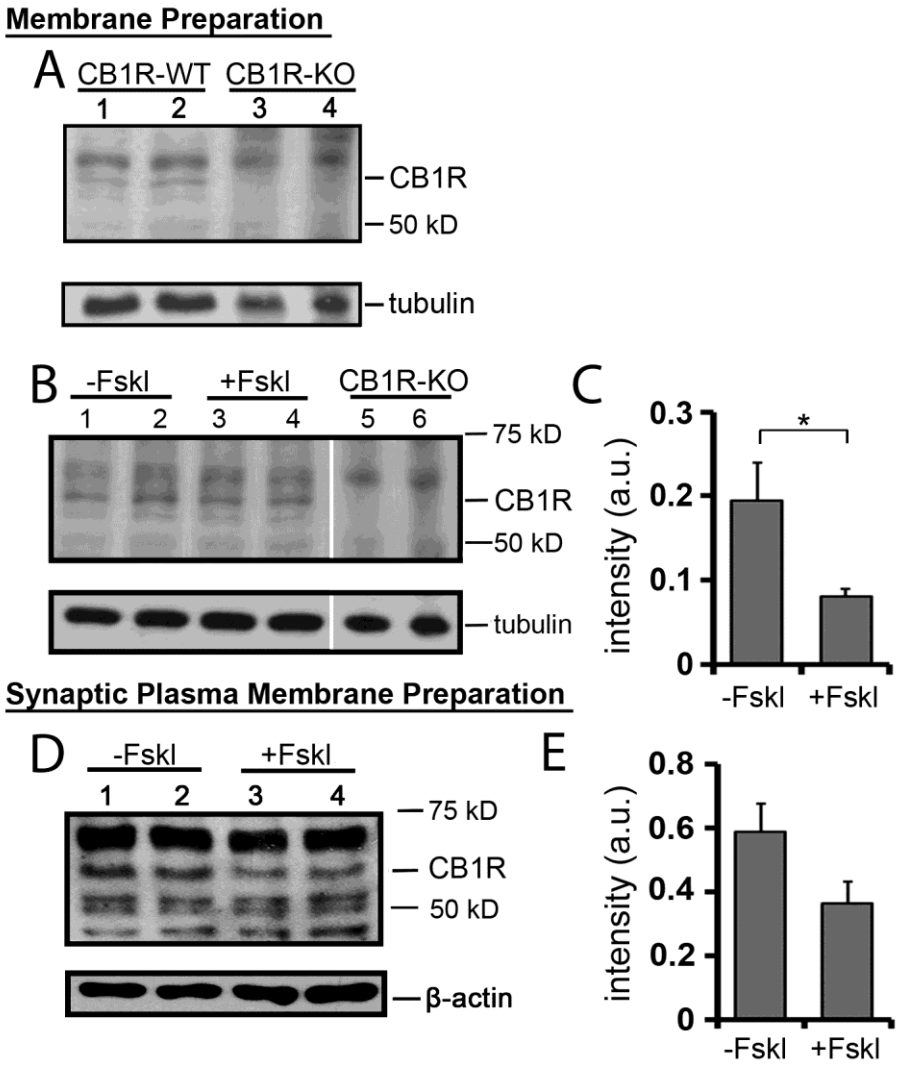

Ying Yang is currently in an eight-year medical education program at Xiangya School of Medicine, Central South University, Changsha, China. She participated in two years of scientific research training at the University of Texas Health Science Center San Antonio, with special interest in presynaptic CB1 receptors at parallel fiber synapses in the cerebellum. She will graduate this summer and start her residency, hoping to be a pain physician and continue her research career in the study of pain.